






Article

Machine Learning for Predicting Fracture Strain in Sheet Metal Forming

Armando E. Marques^{1,2}, Mario A. Dib³, Ali Khalfallah^{1,4,5} , Martinho S. Soares⁶, Marta C. Oliveira^{1,2} , José V. Fernandes^{1,2} , Bernardete M. Ribeiro^{3,7}  and Pedro A. Prates^{1,7,8,*} 

- ¹ CEMMPRE—Centre for Mechanical Engineering, Materials and Processes, Department of Mechanical Engineering, University of Coimbra, 3030-788 Coimbra, Portugal
 - ² ARISE—Advanced Production and Intelligent Systems Associated Laboratory, 4200-465 Porto, Portugal
 - ³ CISUC—Centre for Informatics and Systems of the University of Coimbra, Department of Informatics Engineering, University of Coimbra, 3030-290 Coimbra, Portugal
 - ⁴ Laboratoire de Génie Mécanique, Ecole Nationale d'Ingénieurs de Monastir, Université de Monastir, Monastir 5019, Tunisia
 - ⁵ DGM, Institut Supérieur des Sciences Appliquées et de Technologie de Sousse, Université de Sousse, Sousse 4003, Tunisia
 - ⁶ Toolpresse, Peças Metálicas por Prensagem Lda., 7080-341 Vendas Novas, Portugal
 - ⁷ LASI—Intelligent Systems Associate Laboratory, 4800-058 Guimarães, Portugal
 - ⁸ TEMA—Centre for Mechanical Technology and Automation, Department of Mechanical Engineering, University of Aveiro, 3810-193 Aveiro, Portugal
- * Correspondence: prates@ua.pt; Tel.: +351-234-370-830

Abstract: Machine learning models are built to predict the strain values for which edge cracking occurs in hole expansion tests. The samples from this test play the role of sheet metal components to be manufactured, in which edge cracking often occurs associated with a uniaxial tension stress state at the critical edges of components. For the construction of the models, a dataset was obtained experimentally for rolled ferritic carbon steel sheets of different qualities and thicknesses. Two types of tests were performed: tensile and hole expansion tests. In the tensile test, the yield stress, the tensile strength, the strain at maximum load and the elongation after fracture were determined in the rolling and transverse directions. In the hole expansion test, the strain for which edge cracking occurs, was determined. It is intended that the models can predict the strain at fracture in this test, based on the knowledge of the tensile test data. The machine learning algorithms used were Multilayer Perceptron, Gaussian Processes, Support Vector Regression and Random Forest. The traditional polynomial regression that fits a 2nd order polynomial function was also used for comparison. It is shown that machine learning-based predictive models outperform the traditional polynomial regression method; in particular, Gaussian Processes and Support Vector Regression were found to be the best machine learning algorithms that enable the most robust predictive models.

Keywords: sheet metal forming; machine learning; predictive regression models; fracture strain



Citation: Marques, A.E.; Dib, M.A.; Khalfallah, A.; Soares, M.S.; Oliveira, M.C.; Fernandes, J.V.; Ribeiro, B.M.; Prates, P.A. Machine Learning for Predicting Fracture Strain in Sheet Metal Forming. *Metals* **2022**, *12*, 1799. <https://doi.org/10.3390/met12111799>

Academic Editor: Filippo Berto

Received: 14 September 2022

Accepted: 19 October 2022

Published: 24 October 2022

Publisher's Note: MDPI stays neutral with regard to jurisdictional claims in published maps and institutional affiliations.



Copyright: © 2022 by the authors. Licensee MDPI, Basel, Switzerland. This article is an open access article distributed under the terms and conditions of the Creative Commons Attribution (CC BY) license (<https://creativecommons.org/licenses/by/4.0/>).

1. Introduction

Defects occur very frequently in sheet metal forming, making the process unnecessarily expensive. Thus, the automotive industry, of great importance in the European market, has a permanent need for innovation to guarantee profits and simultaneously ensure that its products meet the requirements of quality, safety, and environmental impact. Currently, more efficient approaches to process design than traditional trial-and-error are being sought. At first, the focus was on the application of the finite element method (FEM) for the simulation of forming processes. This is commonly done resorting to the practical concept of forming limit diagrams (FLDs), introduced to characterize the ductility of metallic sheets subjected to forming operations [1,2]. Originally, the FLD determination was based on an experimental approach, involving the use of metal sheets with different geometries

to reproduce a certain range of monotonic loading paths. However, this experimental approach is both expensive and time consuming, while experience has shown that the obtained FLD presents a very limited usefulness in the formability assessment for processes that are inherently non-linear [3–5].

It is well established that ductile failure in metals occurs due to the presence of defects such as voids and micro-cracks [6]. On the macroscopic scale, damage is observed as the degradation of material properties, e.g., the elastic stiffness, the yield stress or other measurable material properties (see, e.g., [7]). At the microscopic scale, damage evolves by the initiation, growth and coalescence of defects like voids or micro-cracks. This process can lead to the initiation and propagation of macroscopic cracks and to catastrophic failure, which is one reason for the extensive research efforts in this field [8].

During the past three decades, two major damage theories have been developed. One known as continuous damage mechanics (e.g., [7]) is based on the introduction of an internal variable (scalar or tensor) that represents the surface density of the defects. It is also common to include in this category uncoupled models, for which the damage internal variable has no influence on the other plastic internal variables nor the elastic properties of the material and vice versa. In this case, the ductile fracture locus is determined based on the fracture strain evaluated experimentally from tests reproducing a wide range of stress states (e.g., [9]). The other is a physically based micromechanics approach, which tries to reproduce the kinematics of the voids (due to nucleation, growth and coalescence) within the material, for different loading conditions. In this context, Gurson derived a popular model for damage-induced strain softening in metals, from a micromechanical rigid-plastic pore growth model [10]. The related internal variable of the macroscopic constitutive equations is the pore volume fraction, and it has been successfully applied, extended and modified by numerous authors, with the Gurson–Tvergaard–Needleman (GTN) model being the most popular [11]. This model has been subsequently modified to take into account the isotropic and kinematic hardening, as well as strain-path changes (e.g., [12]) and, more recently, plastic anisotropy (e.g., [13]), including tension-compression asymmetry [14]. For further details concerning also the numerical strategies commonly adopted please see, for example [15].

However, the FEM solution alone has limitations related to material variability. Some approaches have been proposed to combine FEM with statistical methods to evaluate the process robustness. These are based on a prior knowledge of the statistical distribution that best describes the variability of each material parameter (e.g., [16,17]). Nevertheless, there can be significant differences in mechanical behaviour between the various sheet metal coils received during the production of a certain component, for which the statistical distribution is unknown. These differences in mechanical behaviour led to the occurrence of defects in the use of some of these coils, which was not predicted during the design process. Robust analysis based on machine learning (ML) algorithms allows the engineer to recognize, monitor and anticipate potential problems that may occur in the production environment due to dispersion. An important feature of robust design in sheet metal forming processes include accurate modelling of the different sources of dispersion, namely material properties, which presupposes the use of representative samples from multiple coils and cast slabs.

Applications of artificial intelligence (AI) techniques have recently been proposed to predict, detect, and classify the occurrence of defects in metal forming processes [18–29]. Among these, there are AI-based techniques that have been used to classify surface defects of hot rolling strips based on techniques such as generative adversarial networks (GAN) [22] and convolutional neural networks (CNN) [23,24], which rely on datasets of collected defects images; CNN-based approaches used to predict the buckling instability of automotive sheet metal panels [25]; machine learning-based techniques used to predict and account for springback in steel and aluminium parts [26–28], as well as for predicting wrinkling [29].

The authors of the current work have previously evaluated the performance of various ML binary classifiers in predicting the occurrence of edge cracking in metal forming processes, exposed to dispersion in the material properties, which yielded satisfactory results [21]. Edge cracking defects refer to the occurrence of fractures in a stamped part, usually at the outer edge of a bent area, where the strain path corresponds to uniaxial tension [21]. In this context, we now seek to evaluate the performance of ML regression algorithms in predicting the occurrence of failure in components obtained from metal forming processes. The main objective is to provide a ML tool capable of performing analysis of sheet metal forming processes, to predict and avoid fracture, which is a very common defect, enabling the increase of the overall productivity considering the dispersion in the mechanical properties. In other words, statistical information on material dispersion is used to predict the strain at fracture, which, if combined with finite element analysis, for example, can allow establishing a predictive approach to component nonconformity. For this purpose, ML models are built to predict the onset of fracture in the hole expansion test, whose sample plays the role of a component to be manufactured, from the knowledge of tensile test results. After this introductory section, the paper is organized as follows: first, the selected regression ML algorithms are described; afterwards, the design procedure to construct and evaluate the predictive ability of the models is described, followed by the results and discussion. Finally, the main conclusions drawn from this work are presented.

2. Regression ML Algorithms

The following subsections present a brief description of each of the ML algorithms used in this work to construct the predictive models; the classic polynomial regression used for comparison is also described.

2.1. Multilayer Perceptron

The Multi-Layer Perceptron (MLP) is one of the most used types of neural networks. It is a feed forward network composed of multiple layers of nodes (neurons), including input, hidden and output layers [30]. The output from a given node of a hidden layer is given by:

$$z_i = \varnothing \left(\sum_j w_{ij} z_j + d_i \right) \quad (1)$$

where z_i is the output from node i of the current layer, z_j is the output from node j of the previous layer, w_{ij} is the weight associated with z_j , d_i is a bias term and \varnothing is a non-linear activation function. For regression problems, the output layer nodes have a similar formulation, but without activation function. The training consists of adjusting the weights to obtain a better fit of the model, through error backpropagation. The weights adjustment is done by increasing (or decreasing) each weight value and then changing all weights in the network accordingly, in an iterative process until a minimum estimate of the prediction error is reached.

2.2. Gaussian Processes

A Gaussian Process (GP) is a collection of random variables that follows a Gaussian distribution and are fully defined by a mean function and a covariance function [31]. The mean function is usually assumed to be zero, and so the covariance function is enough to completely define the GP. The GP regression model can be represented by:

$$y(\mathbf{x}) = f(\mathbf{x}) + \epsilon \quad (2)$$

where $y(\mathbf{x})$ is an observed output for a given set of inputs \mathbf{x} , $f(\mathbf{x})$ is the corresponding GP variable and ϵ represents a Gaussian white noise with zero mean. Assuming that $\mathbf{y}(\mathbf{x}^t)$ is

the target vector of outputs concerning the dataset and $\mathbf{y}(\mathbf{x}^p)$ is the vector of outputs to be predicted, the joint normal probability distribution is given by:

$$\begin{bmatrix} \mathbf{y}(\mathbf{x}^t) \\ \mathbf{y}(\mathbf{x}^p) \end{bmatrix} \sim \mathcal{N}\left(0, \begin{bmatrix} \mathbf{K}(\mathbf{X}, \mathbf{X}) + \sigma_c^2 \mathbf{I} & \mathbf{K}(\mathbf{X}, \mathbf{X}_*) \\ \mathbf{K}(\mathbf{X}_*, \mathbf{X}) & \mathbf{K}(\mathbf{X}_*, \mathbf{X}_*) \end{bmatrix}\right) \quad (3)$$

where σ_c^2 is the noise variance, \mathbf{I} is the identity matrix and each \mathbf{K} is a covariance matrix evaluated for all considered points, with \mathbf{X} representing the training set data, and \mathbf{X}_* the unseen data for which the model will make predictions. Finally, the GP model predictions are given by the following equations:

$$\bar{\mathbf{f}}_* = \mathbf{K}(\mathbf{X}_*, \mathbf{X}) \left[\mathbf{K}(\mathbf{X}, \mathbf{X}) + \sigma_c^2 \mathbf{I} \right]^{-1} \mathbf{y}(\mathbf{x}^t) \quad (4)$$

$$\mathbf{cov}(\mathbf{f}_*) = \mathbf{K}(\mathbf{X}_*, \mathbf{X}_*) - \mathbf{K}(\mathbf{X}_*, \mathbf{X}) \left[\mathbf{K}(\mathbf{X}, \mathbf{X}) + \sigma_c^2 \mathbf{I} \right]^{-1} \mathbf{K}(\mathbf{X}, \mathbf{X}_*) \quad (5)$$

where $\bar{\mathbf{f}}_*$ is the predictions vector (mean), and $\mathbf{cov}(\mathbf{f}_*)$ represents the covariance of model outputs, which acts as a measure of prediction uncertainty.

2.3. Support Vector Regression

The support vector regression (SVR) algorithm fits a function to the available data, while remaining as smooth as possible. This is achieved by considering an error value, γ , under which errors are accepted without penalty [32]. This means finding the function that can encompass the greatest number of training data points in the tube area around it, with a distance of γ or less. Sometimes this is not feasible, and so to give the model some flexibility, soft margins can be defined, in the form of slack variables ζ_i and ζ_i^* . Points at a distance between these variables and γ still affect the shape of the function, but under a penalty. When considering a linear problem, this model is given by:

$$\begin{cases} \min \left(\frac{1}{2} \|\mathbf{w}\|^2 + V \sum_i (\zeta_i + \zeta_i^*) \right) \\ \text{with :} \\ y_i - \mathbf{w}^T \mathbf{x} - b \leq \gamma + \zeta_i \\ \mathbf{w}^T \mathbf{x} + b - y_i \leq \gamma + \zeta_i^* \end{cases} \quad (6)$$

where \mathbf{w} is the normal weight vector to the surface of the approximated function, b is the intercept term and V is a constant representing the trade-off between the tolerance for deviations above γ and the smoothness of the function.

For non-linear problems, this algorithm can be generalized by introducing a kernel trick. A kernel consists of a similarity function between the inputs of the training data and inputs for which the model will make predictions. With a kernel trick, the data is transformed into a higher dimensional space, allowing a linear model to learn non-linear functions without specific mapping.

2.4. Random Forest

Random Forest (RF) is an ensemble model, which consists of a series of decision tree models, each one trained with a randomly generated sample from the training data [33]. A decision tree is generated by applying a continuous splitting process to the training data, based on simple rules that are chosen to minimize an error metric in the resulting nodes [34]. The most common error metric used in this case is the mean squared error (MSE). The splitting process is repeated until each of the resulting final nodes has an MSE below a previously defined threshold, or until all end nodes are below a certain size (regarding the number of training data points that correspond to that node). The predictions from each node correspond to the average of the output values from the training points in the node. The predictions made by a random forest model are the average of the values predicted by each of the decision trees.

2.5. Polynomial Regression

Polynomial regression is a classic parametric modelling technique that fits a multivariate polynomial function to the available training data [35]. The 2nd order polynomial function is used in this work:

$$y^*(\mathbf{x}) = \beta_0 + \sum_{i=1}^p \beta_i x_i + \sum_{i=1}^p \sum_{j>i}^p \beta_{ij} x_i x_j + \sum_{i=1}^p \beta_{ii} x_i^2 \quad (7)$$

where $y^*(\mathbf{x})$ is the estimated response for a given set of inputs \mathbf{x} and β_0 , β_i , β_{ij} and β_{ii} are the set of coefficients (i.e., the model parameters) to be calibrated via traditional least-squares fitting.

3. Design Procedure

This work consists of evaluating the performance of ML regression algorithms in the prediction of strain at the onset of fracture by edge cracking occurring in metal forming components. The following subsections describe the procedure adopted to construct the predictive models, based on a dataset, which was populated with results of mechanical tests, obtained on samples taken from various sheet metal coils; the dataset was used to calibrate the ML algorithms and the performances of the resulting predictive models were evaluated.

3.1. Dataset

The data used in this work consist of experimental results obtained in two different types of mechanical tests: the uniaxial tensile test and the hole expansion test. Uniaxial tensile tests were performed at 0 and 90° with the rolling direction—RD according to ASTM-E8M [36], while hole expansion tests were performed according to ISO 16630 [37]. Uniaxial tension strain paths are present in both types of mechanical tests, similarly to the regions of the components where fracture by edge cracking generally occurs. These tests were performed on 163 samples taken from rolled sheet metal coils, with twelve different thicknesses in the range 0.9 to 8.2 mm, of the same or different type of ferritic carbon steels, i.e., there are 163 entries in the data set. In this context, the scatter of mechanical properties within the same type of steel, often at the origin of component losses due to non-compliance, are also considered.

The results obtained from the tensile tests, at 0 and 90° with RD, are the yield stress (R_e), the ultimate tensile strength (R_m), the corresponding logarithmic strain value (ϵ_{Rm}) and the percentage elongation at fracture for the initial reference length of 50 mm (E_{50}). The minimum, average and maximum values obtained for each variable are presented in Table 1.

Table 1. Distribution of the tensile test results.

	$R_{e,0^\circ}$ [MPa]	$R_{e,90^\circ}$ [MPa]	$R_{m,0^\circ}$ [MPa]	$R_{m,90^\circ}$ [MPa]	$\epsilon_{Rm,0^\circ}$ [-]	$\epsilon_{Rm,90^\circ}$ [-]	$E_{50,0^\circ}$ [%]	$E_{50,90^\circ}$ [%]
Minimum	138.6	137.30	257.1	262.0	0.074	0.054	9.0	11.0
Maximum	577.9	630.1	615.6	675.0	0.251	0.260	51.0	52.0
Mean	340.0	356.8	416.5	423.8	0.156	0.146	29.1	28.1
Std. dev.	122.0	135.0	105.3	113.6	0.004	0.046	10.8	11.3

Figure 1 represents all possible relationships between the variables in Table 1. There are some linear correlations between the values of the stress results, namely between $R_{e,0^\circ}$, $R_{e,90^\circ}$, $R_{m,0^\circ}$ and $R_{m,90^\circ}$, which present R^2 correlation values between 0.95 and 0.98. For the remaining representations, i.e., involving only one or even no stress and the remaining results ($\epsilon_{Rm,0^\circ}$, $\epsilon_{Rm,90^\circ}$, $E_{50,0^\circ}$, $E_{50,90^\circ}$), no significant correlation can be found.

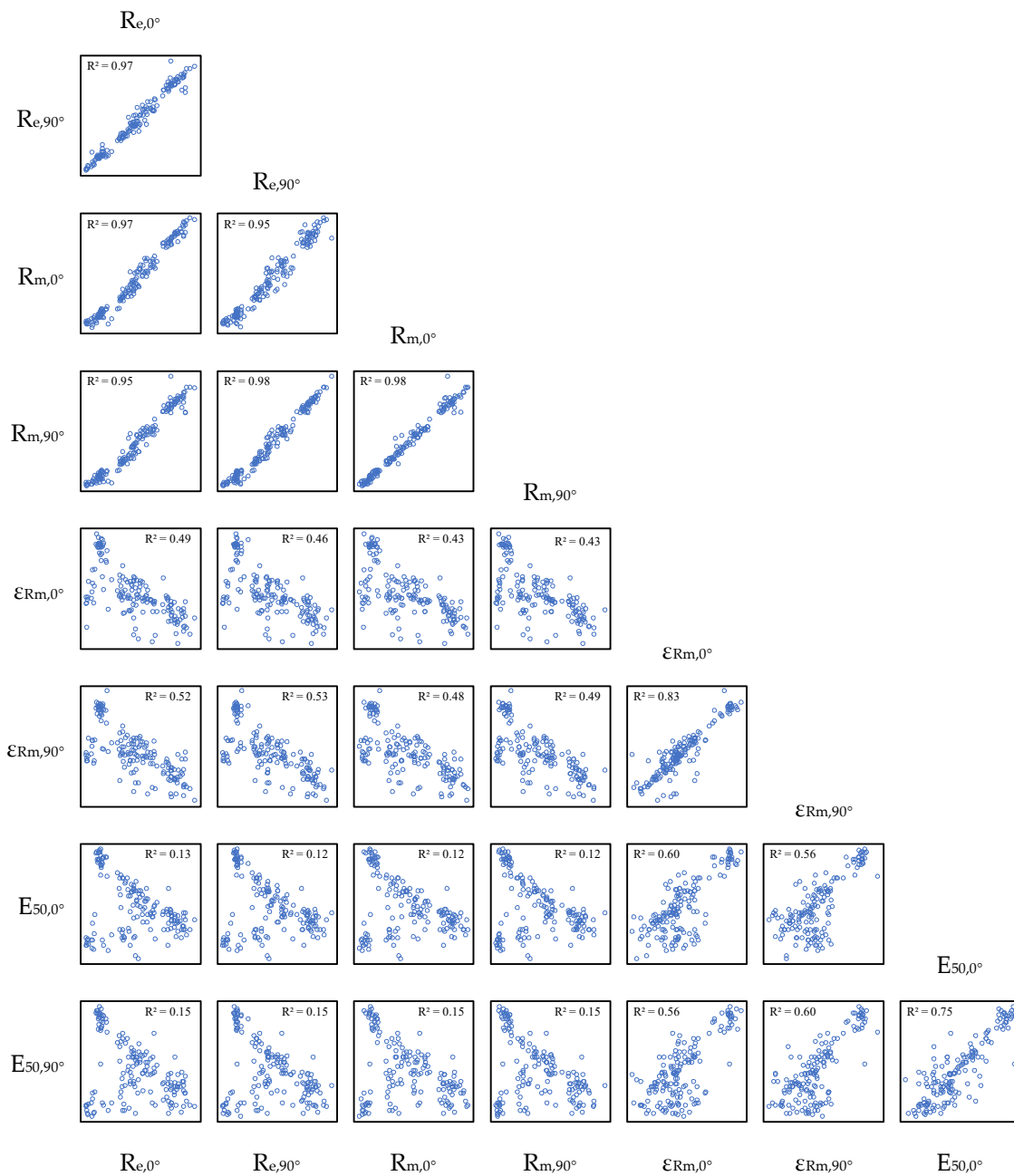


Figure 1. Representation of the relationships between the obtained tensile test results, defined in Table 1.

The samples used for the hole expansion tests (HET) had an initial hole diameter of 20 mm, the burr was positioned in the freely expanding side during the HET and the tests were carried out up to values of punch displacement that ensured the fracture of all samples. The result obtained from these tests is the logarithmic circumferential (hoop) strain at fracture, ϵ_f . Figure 2 shows the distribution of logarithmic strain values at fracture obtained for the hole expansion tests.

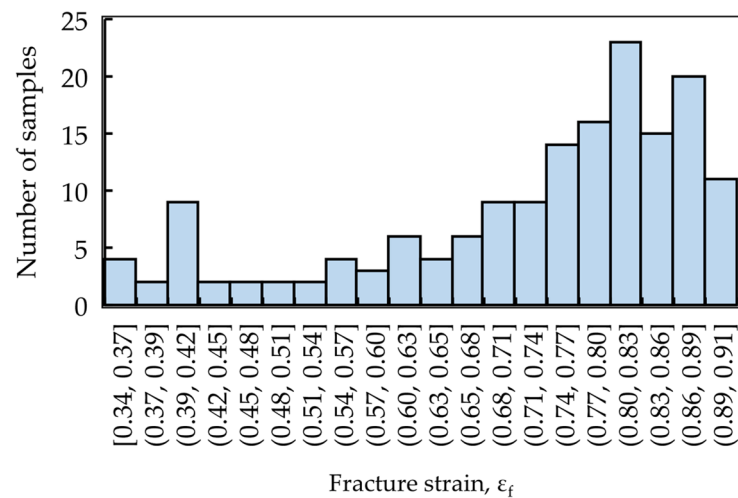


Figure 2. Distribution of the strain values at fracture, ϵ_f , obtained for the hole expansion tests.

The relationships between the fracture strain values, ϵ_f , in the hole expansion test and the tensile test results are shown in Figure 3. No obvious correlation was found.

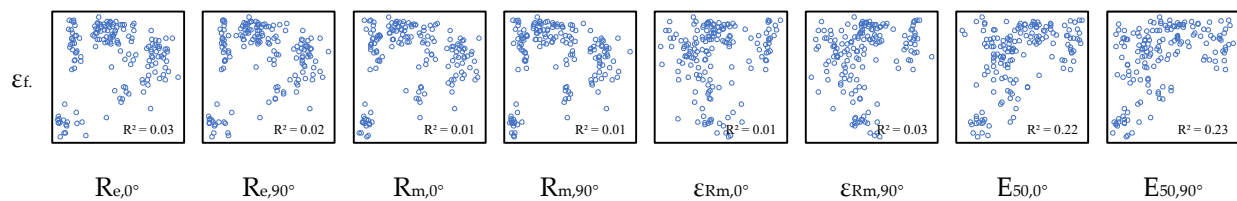


Figure 3. Fracture strain in HET as a function of the results obtained from the tensile test, defined in Table 1.

3.2. Model Calibration

The predictive models were constructed using the following regression ML algorithms: (i) Multilayer Perceptron (MLP); (ii) Gaussian Process (GP); (iii) Support Vector Regression (SVR); (iv) Random Forest (RF). Predictive models based on classic polynomial regression were also constructed, for comparison. The ML-based predictive models were generated with python libraries, specifically, GPy for GP [38] and Scikit-learn for the other ML algorithms [39]. To properly evaluate the predictive performance of the models created by the various algorithms, the dataset is divided into a training set and a testing set. The training and testing sets were randomly generated, with the training set containing 70% of the data and the testing set the remaining 30%. Data scaling was performed in all the data. An important step in the training process of the ML models is the optimisation of hyperparameters. This was based on an iterative trial-and-error approach, in which the training set is split again into a temporary training set containing 70% of the data, and a calibration set containing the remaining 30%. This split is done randomly, 30 times, and for each model, trained with the temporary training set, predictions are made for the validation set and the predictive performance is evaluated. The set of hyperparameters that leads to the best performances across the 30 data splits are shown in Table 2. For some algorithm hyperparameters, there are a finite number of possibilities, this is the case of the choice of kernel to use for the GP or SVR algorithms, for example; on the other hand, some hyperparameters have endless possibilities, such as the number of nodes in an MLP layer, or the value of the C parameter for the SVR algorithm. For the hyperparameters with a finite number of possibilities, all possibilities were considered (except for the GP algorithm, since the GPy library has many kernel formulations available, and only the RBF, Matern32 and Matern52 kernels were tested). For the remaining hyperparameters, specific values were selected (e.g., the number of nodes in each layer of an MLP model, where the values 2,

4, 6, 8 and 10 were tested). For the MLP algorithm, the hyperparameters considered were the number of layers (ranging from 1 to 3), the number of nodes in each layer (ranging from 3 to 20), the alpha value (ranging from 0.0001 to 0.005), the choice of activation function (tanh, logistic or relu) and the choice of the solver (lbfgs or adam). The chosen set of hyperparameters has 3 layers, in a configuration of (6, 4, 4) nodes, with an alpha value of 0.0001, the tanh activation function and using the adam solver. For the GP algorithm, the hyperparameters considered were the kernel function (RBF, Matern32 or Matern52) and the optimiser function (lbfgs or tnc). The kernel function chosen was the RBF function and the optimiser chosen was lbfgs. For the SVR algorithm, the hyperparameters considered were the kernel function (RBF or polynomial), the value of C (ranging from 0 to 2) and the epsilon value (ranging from 0.001 to 0.2). The hyperparameter configuration chosen consists of the RBF kernel, with a C value of 0.5 and an epsilon of 0.01. For the RF algorithm, the hyperparameters considered were the number of estimators (ranging from 100 to 1000), the choice of splitting criterion (squared_error or absolute_error) and min_samples_leaf (ranging from 1 to 3). The chosen set of hyperparameters consists of 1000 estimators, using the squared_error criterion and a min_sample_leaf of 1.

Table 2. Hyperparameter values set for the ML algorithms MLP, GP, SVR and RF.

	Number of Layers	Nodes Per Layer	Alpha	Activation Function	Solver
MLP	3	6/4/4	0.0001	Tanh	Adam
	Kernel function	Optimiser function			
GP	RBF	lbfgs			
	Kernel function	C	Epsilon		
SVR	RBF	0.5	0.01		
	Number of estimators	Splitting criterion	Min_samples_leaf		
RF	1000	Squared_error	1		

3.3. Performance Evaluation

The predictive performance evaluation is based on four metrics. The first metric is the root mean square relative error (RMSRE), which is given by:

$$\text{RMSRE} = \sqrt{\frac{1}{j} \sum_{i=1}^j \left(\frac{y_i - y_i^*}{y_i} \right)^2} \quad (8)$$

where y and y^* are the measured and predicted response values for the output variables, respectively, and j is the number of test points.

The second metric is the maximum absolute error, which is given by:

$$\text{max error} = \max_i |y_i - y_i^*| \quad (9)$$

The third metric is the mean absolute error (MAE), which is given by:

$$\text{MAE} = \frac{1}{j} \sum_{i=1}^j |y_i - y_i^*| \quad (10)$$

The last metric is the R-square value, given by:

$$R^2 = 1 - \frac{\sum_{i=1}^j (y_i - y_i^*)^2}{\sum_{i=1}^j (y_i - \bar{y})^2} \quad (11)$$

where \bar{y} is the average of the measured response values of the output variables. This metric expresses the extent to which the variance of the output variables is explained by the independent variables in the model, which indicates how likely the model is to make good predictions for unseen data.

4. Results and Discussion

In order to evaluate the performance of the ML algorithms mentioned above, the result set of the 163 different materials was randomly split into two groups (one referring to 115 (70%) materials, used for training, and the other to 48 (30%), used for test); the choice of materials for each group was performed randomly, in 15 different ways, which are now called cases under analysis. The analysis consists of predicting the fracture strain value in the hole expansion test based on the tensile test results referred to in Table 1 and Figure 1, respectively. Figure 4 shows an illustrative example of the results obtained by the different ML algorithms and the 2nd order polynomial regression, comparing the prediction of the strain at fracture in the HET with the experimentally measured; this figure also presents the predictive performances according to the different metrics considered, for the specific case under analysis (see also Table 3). It shows that the ML algorithms provide better fracture strain predictions than traditional 2nd order polynomial regression. GP is the ML algorithm with the best performance, presenting the lowest values of RMSRE (=0.145), max error (=0.296) and MAE (=0.060), and the highest R^2 value (=0.67); in contrast, polynomial regression presents the highest values of RMSRE (=0.28), max error (=0.62) and MAE (=0.13), and the lowest R^2 value (=−0.63).

Table 3. Performance metrics values corresponding to Figure 4f.

	MLP	GP	SVR	RF	RSM
RMSRE	0.191	0.145	0.150	0.203	0.280
Max. Error	0.440	0.296	0.301	0.324	0.619
MAE	0.091	0.058	0.062	0.068	0.125
R^2	0.206	0.687	0.650	0.481	−0.630

As previously mentioned, the predictive models were tested for 15 random splits (70% for training + 30% for test), to assess the extent to which the model performances are influenced by the choice made, even if randomly. The overall results of this robustness evaluation are shown in Figure 5 (see also Table 4). This figure confirms that GP and SVR are the best performing ML algorithms, leading to more robust predictive models than MLP and RF algorithms and the traditional 2nd order polynomial regression. Although the performance and robustness of both GP and SVR algorithms is significantly superior to RSM, they still have a predictive capability that could be improved (for example, the average value of R^2 is currently close to 0.5). If the dataset is enriched over time, as new sheet metal coils become available during production, it is expected that the predictive capability and robustness of ML algorithms will gradually improve.

Table 4. Performance metrics values corresponding to Figure 5f.

		MLP	GP	SVR	RF	RSM
RMSRE	Mean	0.180	0.156	0.164	0.187	0.274
	Std. Dev.	0.031	0.022	0.033	0.030	0.038
Max. Error	Mean	0.336	0.273	0.288	0.324	0.494
	Std. Dev.	0.083	0.039	0.045	0.062	0.103
MAE	Mean	0.091	0.072	0.071	0.080	0.123
	Std. Dev.	0.014	0.008	0.008	0.012	0.017
R^2	Mean	0.202	0.460	0.474	0.278	−0.604
	Std. Dev.	0.439	0.316	0.280	0.418	0.950

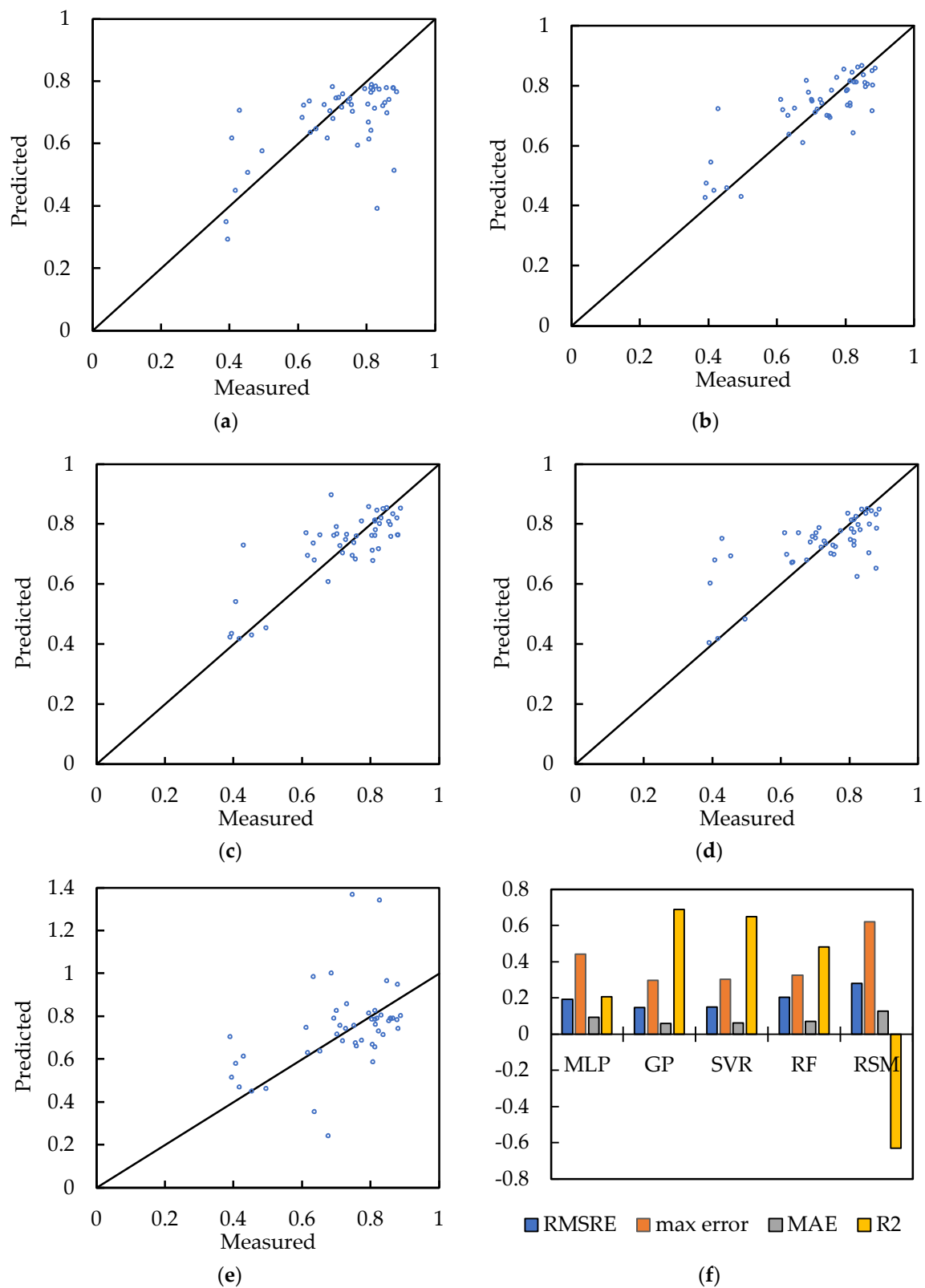


Figure 4. Prediction of fracture strain in the HET as a function of the respective measured value (illustrative example for one of the 15 cases analysed): (a) MLP; (b) GP; (c) SVR; (d) RF; (e) 2nd order polynomial regression; (f) performance metrics (see also Table 3).

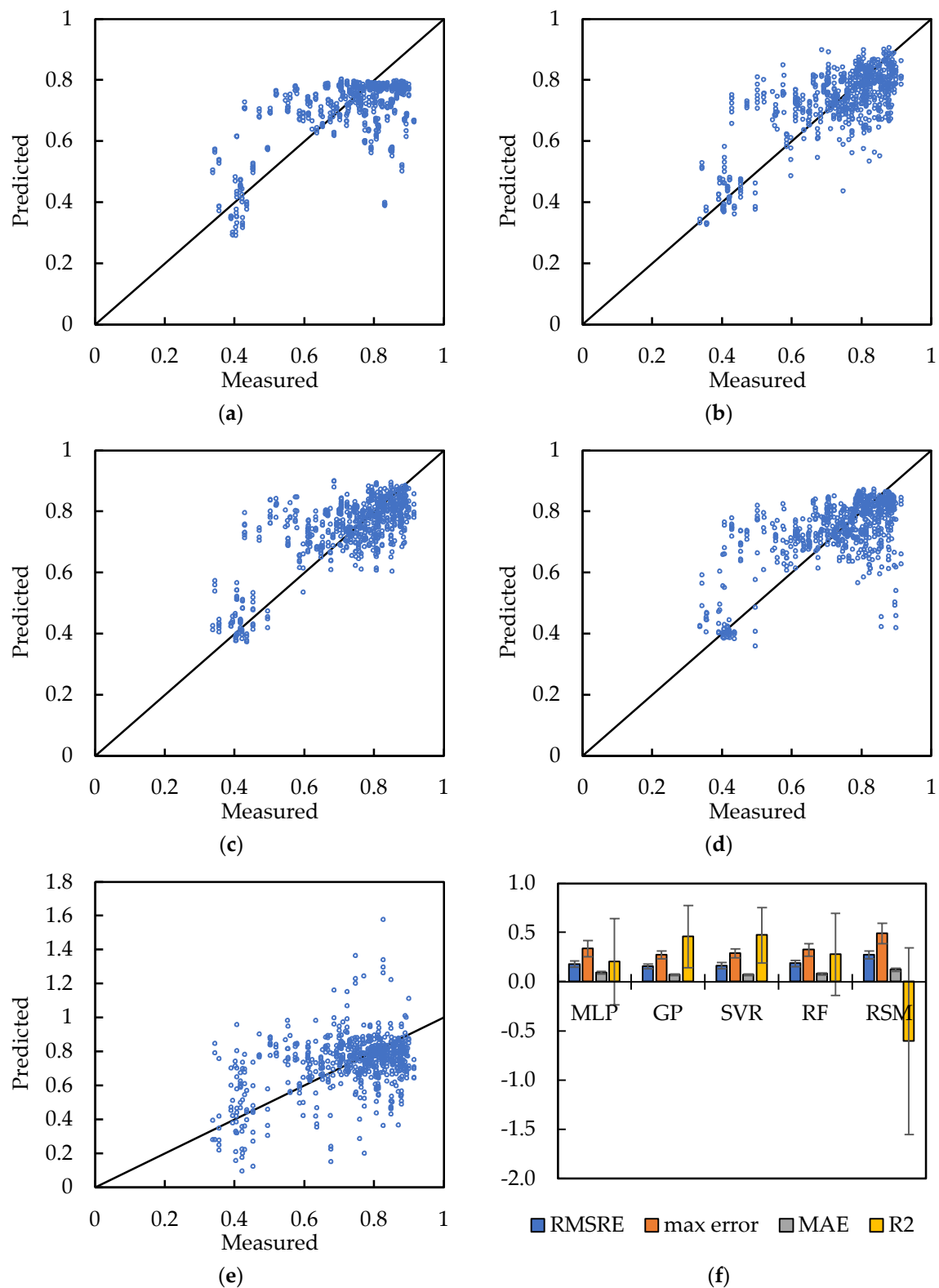


Figure 5. Prediction of fracture strain in the HET as a function of the respective measured value, for all 15 cases analysed: (a) MLP; (b) GP; (c) SVR; (d) RF; (e) 2nd order polynomial fitting; (f) performance metrics (see also Table 4).

5. Conclusions

This work deals with the performance of various ML regression algorithms in predicting fracture strain values related to the onset of edge cracking in sheet metal forming processes. The aim was to predict the fracture strain value in the hole expansion test from the knowledge of tensile test results, considering that edge cracking often occurs associated with a uniaxial tension stress state at the critical edges of components. For this purpose, a dataset was firstly created, containing experimental results of both tests, then predictive models were constructed and, finally, their performance was evaluated and compared. In general, the performance of ML algorithms is clearly superior to traditional polynomial regression modelling technique. In general, the ML algorithms can predict the onset of edge cracking satisfactorily. GP and SVR algorithms were found to be capable machine learning algorithms that enable robust predictive models. Their application in an industrial environment is recommended, as it can certainly contribute to the reduction of production costs and scrap rates. In this regard, the prediction results can be applied to sheet metal forming processes, since edge cracking often occurs associated with a uniaxial tension stress state at the critical edges of components. For example, finite element simulations of the real forming process can be used to estimate the strain at critical edges of the component. So, if this estimated strain exceeds the fracture strain predicted by the ML model, it is likely that edge cracks will occur in real forming processes.

Author Contributions: Conceptualization, J.V.F. and P.A.P.; formal analysis, A.E.M., A.K. and M.A.D.; funding acquisition, J.V.F., M.C.O. and P.A.P.; investigation, A.E.M., A.K., M.A.D., J.V.F. and P.A.P.; software, B.M.R.; supervision, B.M.R., J.V.F., M.C.O. and P.A.P.; writing—original draft, A.E.M., J.V.F. and P.A.P.; writing—review and editing, A.E.M., A.K., B.M.R., J.V.F., M.A.D., M.C.O., M.S.S. and P.A.P.; resources, M.S.S., J.V.F. and P.A.P. All authors have read and agreed to the published version of the manuscript.

Funding: This research was sponsored by FEDER funds through the program COMPETE (Programa Operacional Factores de Competitividade), by national funds through FCT (Fundação para a Ciência e a Tecnologia) under the projects UIDB/00285/2020, UIDB/00326/2020, UIDB/00481/2020, UIDP/00481/2020, CENTRO-01-0145-FEDER-022083, LA/P/0104/2020 and LA/P/0112/2020; this research was also co-funded by POCI under the projects PTDC/EME-EME/31243/2017 (RDFORMING) and PTDC/EME-EME/31216/2017 (EZ-SHEET).

Conflicts of Interest: The authors declare no conflict of interest.

References

1. Keeler, S.P.; Backofen, W.A. Plastic instability and fracture in sheets stretched over rigid punches. *Trans. Am. Soc. Met.* **1963**, *56*, 25–48.
2. Goodwin, G.M. Application of strain analysis to sheet metal forming problems in the press shop. *SAE Trans.* **1968**, *77*, 380–387.
3. Stoughton, T.B.; Zhu, X. Review of theoretical models of the strain-based FLD and their relevance to the stress-based FLD. *Int. J. Plast.* **2004**, *20*, 1463–1486. [[CrossRef](#)]
4. Graf, A.; Hosford, W. Effect of changing strain paths on forming limit diagrams of AI 2008-T4. *Metall. Mater. Trans. A* **1993**, *24*, 1993–2503. [[CrossRef](#)]
5. Abedini, A.; Butcher, C.; Worswick, M.J. Experimental fracture characterisation of an anisotropic magnesium alloy sheet in proportional and non-proportional loading conditions. *Int. J. Solids Struct.* **2018**, *144–145*, 1–19. [[CrossRef](#)]
6. McClintock, F.A. A criterion for ductile fracture by the growth of holes. *J. Appl. Mech.* **1968**, *35*, 363. [[CrossRef](#)]
7. Lemaitre, J. *A Course on Damage Mechanics*; Springer: Berlin/Heidelberg, Germany, 1996; ISBN 978-3-540-60980-3.
8. Wulfinghoff, S.; Fassin, M.; Reese, S. A damage growth criterion for anisotropic damage models motivated from micromechanics. *Int. J. Solids Struct.* **2017**, *121*, 21–32. [[CrossRef](#)]
9. Pack, K.; Tancogne-Dejean, T.; Gorji, M.B.; Mohr, D. Hosford-Coulomb ductile failure model for shell elements: Experimental identification and validation for DP980 steel and aluminum 6016-T4. *Int. J. Solids Struct.* **2018**, *151*, 214–232. [[CrossRef](#)]
10. Gurson, A.L. Continuum theory of ductile rupture by void nucleation and growth: Part I—Yield criteria and flow rules for porous ductile media. *J. Eng. Mater. Technol.* **1977**, *99*, 2. [[CrossRef](#)]
11. Needleman, A.; Tvergaard, V. An analysis of ductile rupture modes at a crack tip. *J. Mech. Phys. Solids* **1987**, *35*, 151–183. [[CrossRef](#)]
12. Besson, J.; Guillemer-Neel, C. An extension of the Green and Gurson models to kinematic hardening. *Mech. Mater.* **2003**, *35*, 1–18. [[CrossRef](#)]

13. Benzerga, A.A.; Besson, J.; Pineau, A. Anisotropic ductile fracture: Part II: Theory. *Acta Mater.* **2004**, *52*, 4639–4650. [[CrossRef](#)]
14. Cazacu, O.; Stewart, J.B. Analytic plastic potential for porous aggregates with matrix exhibiting tension–compression asymmetry. *J. Mech. Phys. Solids* **2009**, *57*, 325–341. [[CrossRef](#)]
15. Fincato, R.; Tsutsumi, S. Ductile fracture modeling of metallic materials: A short review. *Frat. Integr. Strutt.* **2022**, *59*, 1–17. [[CrossRef](#)]
16. De Souza, T.; Rolfe, B.F. Characterising material and process variation effects on springback robustness for a semi-cylindrical sheet metal forming process. *Int. J. Mech. Sci.* **2010**, *52*, 1756–1766. [[CrossRef](#)]
17. Wiebenga, J.H.; Atzema, E.H.; An, Y.G.; Vegter, H.; van den Boogaard, A.H. Effect of material scatter on the plastic behavior and stretchability in sheet metal forming. *J. Mater. Process Technol.* **2014**, *214*, 238–252. [[CrossRef](#)]
18. Tercan, H.; Meisen, T. Machine learning and deep learning based predictive quality in manufacturing: A systematic review. *J. Intell. Manuf.* **2022**, *33*, 1879–1905. [[CrossRef](#)]
19. Marques, A.E.; Prates, P.A.; Pereira, A.F.G.; Oliveira, M.C.; Fernandes, J.V.; Ribeiro, B.M. Performance comparison of parametric and non-parametric regression models for uncertainty analysis of sheet metal forming processes. *Metals* **2020**, *10*, 457. [[CrossRef](#)]
20. Dib, M.A.; Oliveira, N.J.; Marques, A.E.; Oliveira, M.C.; Fernandes, J.V.; Ribeiro, B.M.; Prates, P.A. Single and ensemble classifiers for defect prediction in sheet metal forming under variability. *Neural. Comput. Appl.* **2020**, *32*, 12335–12349. [[CrossRef](#)]
21. Marques, A.E.; Prates, P.A.; Fonseca, A.R.; Oliveira, M.C.; Soares, M.S.; Fernandes, J.V.; Ribeiro, B.M. Machine learning for the prediction of edge cracking in sheet metal forming processes. In *Machine Learning and Artificial Intelligence with Industrial Applications. Management and Industrial Engineering*, 1st ed.; Carou, D., Sartal, A., Davim, J.P., Eds.; Springer: Cham, Switzerland, 2022; pp. 127–144. [[CrossRef](#)]
22. Hao, Z.; Li, Z.; Ren, F.; Lv, S.; Ni, H. Strip steel surface defects classification based on Generative Adversarial Network and Attention Mechanism. *Metals* **2022**, *12*, 311. [[CrossRef](#)]
23. Boudiaf, A.; Harrar, K.; Benlahmidi, S.; Zaghdoudi, R.; Ziani, S.; Taleb, S. Automatic surface defect recognition for hot-rolled steel strip using AlexNet convolutional neural network. In Proceedings of the 7th International Conference on Image and Signal Processing and their Applications, Mostaganem, Algeria, 8–9 May 2022. [[CrossRef](#)]
24. Wang, D.; Xu, Y.; Duan, B.; Wang, Y.; Song, M.; Yu, H.; Liu, H. Intelligent recognition model of hot rolling strip edge defects based on deep learning. *Metals* **2021**, *11*, 223. [[CrossRef](#)]
25. Lee, S.; Quagliato, L.; Park, D.; Berti, G.A.; Kim, N. A buckling instability prediction model for the reliable design of sheet metal panels based on an artificial intelligent self-learning algorithm. *Metals* **2021**, *11*, 1533. [[CrossRef](#)]
26. Miranda, S.S.; Barbosa, M.R.; Santos, A.D.; Pacheco, J.B.; Amaral, R.L. Forming and springback prediction in press brake air bending combining finite element analysis and neural networks. *J. Strain. Anal. Eng. Des.* **2018**, *53*, 584–601. [[CrossRef](#)]
27. Spathopoulos, S.C.; Stavroulakis, G.E. Springback prediction in sheet metal forming, based on finite element analysis and artificial neural network approach. *Appl. Mech.* **2020**, *1*, 97–110. [[CrossRef](#)]
28. Liu, S.; Xia, Y.; Shi, Z.; Yu, H.; Li, Z.; Lin, J. Deep learning in sheet metal bending with a novel theory-guided deep neural network. *IEEE/CAA J. Autom. Sin.* **2021**, *8*, 565–581. [[CrossRef](#)]
29. Zhang, S.; Yuan, Y.; Wang, Z.; Lin, Y.; Jiang, L.; Fu, M. A hierarchical prediction method based on hybrid-kernel GWO-SVM for metal tube bending wrinkling detection. *Int. J. Adv. Manuf. Technol.* **2022**, *121*, 5329–5342. [[CrossRef](#)]
30. Silva, C.; Ribeiro, B. *Aprendizagem Computacional em Engenharia*, 1st ed.; Imprensa da Universidade de Coimbra: Coimbra, Portugal, 2018; pp. 27–66. [[CrossRef](#)]
31. Lin, D.J.; Huang, L.; Zhou, H.B. Forming defects prediction for sheet metal forming using Gaussian process regression. In Proceedings of the 29th Chinese Control and Decision Conference, Chongqing, China, 28–30 May 2017. [[CrossRef](#)]
32. Smola, A.J.; Schölkopf, B.A. Tutorial on support vector regression. *Stat. Comput.* **2014**, *14*, 199–222. [[CrossRef](#)]
33. Breiman, L. Random forests. *Mach. Learn.* **2001**, *45*, 5–32. [[CrossRef](#)]
34. Kaur, D.; Wilson, D.; Forrest, M.; Feng, L. Regression tree and neuro-fuzzy approach to system identification of laser tap welding. In Proceedings of the 2005 Annual Meeting of the North American Fuzzy Information Processing Society, Detroit, CA, USA, 26–28 June 2005. [[CrossRef](#)]
35. Sun, G.; Li, G.; Li, Q. Variable fidelity design based surrogate and artificial bee colony algorithm for sheet metal forming process. *Finite. Elem. Anal. Des.* **2012**, *59*, 76–90. [[CrossRef](#)]
36. *ASTM E8/E8M-08*; E8M-08 Standard Test Methods for Tension Testing of Metallic Materials. ASTM International: West Conshohocken, PA, USA, 2008.
37. *ISO 16630*; Metallic Materials—Sheet and Strip—Hole Expanding Test. International Organization for Standardization: Geneva, Switzerland, 2017.
38. GPy: A Gaussian Process Framework in Python. Available online: <http://github.com/SheffieldML/GPy> (accessed on 26 November 2021).
39. Pedregosa, F.; Varoquaux, G.; Gramfort, A.; Michel, V.; Thirion, B.; Grisel, O.; Blondel, M.; Prettenhofer, P.; Weiss, R.; Dubourg, V. Scikit-learn: Machine learning in Python. *J. Mach. Learn. Res.* **2011**, *12*, 2825–2830. [[CrossRef](#)]